Numerical simulation of leakage rates of labyrinth seal in reciprocating compressor

H N Tang[1, 3], H Yao[2], S J Wang[1], X S Meng[1], H T Qiao[1] and J H Qiao[1]

[1] School of Mechanical Engineering, Shenyang University of Technology, Shenyang, China
[2] AVIC Aerodynamic Research Institute, Shenyang, China

Email: 28775147@qq.com

Abstract. The influence of labyrinth seal structure on leakage behaviour in a reciprocating compressor was addressed in this paper. The effects of the main labyrinth seal parameters, such as tooth angle, sealing clearance, and cavity depth, were compared using FLUENT software and iterative calculation results. Simulations of the sealing process with the influence of internal structure size of labyrinth seal performance in different structures were conducted to explore the characteristics of fluid flow. By comparing the simulations of leakage of fluid-structure interaction and experience formula calculations, the results revealed the validity of the fluid-structure interaction analysis method. The CFD analysis method for fluid-structure coupling was adopted to verify the theory of labyrinth seals and for the design of a labyrinth structure.

1. Introduction

As a kind of non-contact dynamic seal, labyrinth seals are composed of a series of throttling backlash and expansion cavities. A labyrinth seal reduces the leakage rate by increasing the local kinetic energy loss of fluid flow to improve the sealing performance. Widely used in centrifugal compressors, turbine coolers, turbine expansion engines, and other mechanical applications, labyrinth seals do not need lubrication, offer stable and reliable performance, and are convenient [1-4]. Through the variation of cavity expansion, local kinetic energy of the fluid flow is incrementally lost in a labyrinth seal. Currently, due to the strict requirements of the materials, difficulty of manufacturing, high standards of mechanical processing, and assembly accuracy, labyrinth seals are produced by only a small number of companies, such as Swiss Sulzer, throughout the world. The Sulzer company has produced labyrinth compressors since 1935, accounting for about ninety percent of the world market production. Japan Steel Works, Germany's Linde, and only a few other companies produce labyrinth compressors, and their products are mainly used to satisfy the internal demands of their enterprise groups. How to effectively reduce leakage is one of the key technical problems afflicting labyrinth sealing technology. To date, many research projects have made progress on design optimization of labyrinth compressors, but the mechanism of labyrinth seals, which play a decisive role in the production capacity of labyrinth compressors, has not yet been perfected.

Presently, calculating leakage rates is conducted by utilizing FLUENT software to analyze flow fields independently [5-7]. Research methods mainly involve CFD numerical analysis, thermodynamic theory analysis, leakage measurement and flow visualization, and the analysis method combining numerical simulation and experimental analysis. Toff adopted the FDM numerical analysis method to

perform numerical simulations on incompressible flow fields with a straight-through labyrinth seal structure, and Versteeg et al. used the same approach [8, 9]. Rhode and Bobolink first simulated [10].

2. Selection of leakage rate algorithm

There are several methods for calculating leakage rates of labyrinth seals including the Martin, Sodalist, Egli, Dumbarton, and Vermes calculation methods. These algorithms, based on specific types of labyrinth seals, are suitable for different applications. Presently, geometric analysis of labyrinth seals is primarily based on two- or three-dimensional flow motion equations, which simplifies the calculation model of seal flow fields. As such, it is not possible to accurately obtain the internal flow field of a seal and pressure field distribution under the interplay of an actual flow field and solid wall. There is interaction between the piston reciprocating movement and gas, which means that the piston reciprocating movements affect the pressure distribution of the gas flow field. Meanwhile, the internal flow field structure is also changed by the gas forces on the piston. Consequently, the pressure distribution of the gas is influenced. Because there is the potential for significant errors if these aspects are studied separately, combining the two problems in fluid-solid coupling can obtain more accurate results.

The flow discipline of leakage fluid inside the seal cavity follows the mass, energy, and momentum conservation formulas. The following general form can be derived by the general variable ϕ [8]:

$$\frac{\partial(\mathrm{p}\phi)}{\partial \mathrm{t}}+\mathrm{div}(\rho \mathrm{u}\phi)=\mathrm{div}(\varphi \mathrm{grad}\phi)+s \tag{1}$$

The formula can be expanded as follows:

$$\begin{aligned}&\frac{\partial(\rho\phi)}{\partial \mathrm{t}}+\frac{\partial(\rho \mathrm{u}\phi)}{\partial \mathrm{x}}+\frac{\partial(\rho \mathrm{v}\phi)}{\partial y}+\frac{\partial(\rho w\phi)}{\partial \mathrm{z}}\\&=\frac{\partial}{\partial x}\left(\varphi\frac{\partial\phi}{\partial x}\right)+\frac{\partial}{\partial y}\left(\varphi\frac{\partial\phi}{\partial y}\right)+\frac{\partial}{\partial z}\left(\varphi\frac{\partial\phi}{\partial z}\right)+s\end{aligned} \tag{2}$$

where ϕ, φ, and S are the general variable, generalized diffusion coefficient, and generalized source term, respectively.

In light of the general equation, the following iterative calculation approach was applied to obtain an equation for theoretical leakage rates of labyrinth seals [9]:

$$G_{\mathrm{i}}=\gamma_{\mathrm{i}} A\sqrt{\frac{2\mathrm{k}}{\mathrm{k}-1}}\frac{P_{\mathrm{i}-1}}{\sqrt{RT_0}}g(\lambda_i) \tag{3}$$

In Eq. (3), i= 1,2,…,n.

Expressly, $\mathrm{g}(\lambda_i)=-3.0495+7.599\lambda_i+(-7.014)\lambda_i^{\,2}+2.945\lambda_i^{\,3}+(-0.462)\lambda_i^{\,4}$ (4)

$$\mathrm{g}(\lambda_i)=-3.0495+7.599\lambda_i-7.014\lambda_i^{\,2}+2.945\lambda_i^{\,3}-0.462\lambda_i^{\,3} \tag{5}$$

$$\gamma_i=\sqrt{\frac{n}{(1-J)n+1}} \tag{6}$$

$$J=1-\left(1+16.6\frac{h}{L}\right)^{-2} \tag{7}$$

$$\lambda_{\mathrm{i}}=\frac{P_{i-1}}{P_i} \tag{8}$$

where A is the cross-sectional area, K is the gas adiabatic index, n is the sealing teeth number; h is the gap width of the sealing tooth mouth, L is the gap of the two adjacent teeth, and λ_{i} is the pressure ratio.

Because the kinetic energy overload effect of a staggered labyrinth seal is smaller, r_{i} was set as 1 directly.

In order to determine which $k-\varepsilon$ turbulence model to use for this research, the calculation results of three $k-\varepsilon$ turbulence models from literature were compared [11]. The results of the standard $k-\varepsilon$ model were determined to be closer to the actual experiment. Therefore, in this paper, the standard $k-\varepsilon$ model was used as the turbulence model.

In the standard $k-\varepsilon$ model, the eddy viscosity model of Reynolds stress was as follows [12]:

$$\tau_{ij} = -\rho\overline{uu}_j = 2u_t\left(S_{ij} - \frac{S_{nn}\delta_{ij}}{3}\right) - \frac{2\rho k\delta_{ij}}{3} \tag{9}$$

$$u_t = c_u f_u \rho k^2 / \varepsilon \tag{10}$$

$$\varepsilon = \frac{\mu}{\rho}\overline{\left(\frac{\partial \mathrm{u}_1'}{\partial x_k}\right)\left(\frac{\partial \mathrm{u}_1'}{\partial x_k}\right)} \tag{11}$$

where u_t is eddy viscosity, S_{ij} is the strain rate tensor of average velocity, δ_{ij} is the kronecker operator, and K is the turbulent kinetic energy.

In the rectangular coordinate system, the governing equation of the standard $k-\varepsilon$ model is as follows for K equation (turbulent kinetic energy equation):

$$\frac{\partial \rho k}{\partial t} + \frac{\partial\left(\rho u_j k\right)}{\partial x_j} = \frac{\partial}{\partial x_j}\left[\left(\mu + \frac{u_t}{\sigma_k}\right)\frac{\partial k}{\partial x_j}\right] + G_k + G_b - \rho\varepsilon - Y_M + S_k \tag{12}$$

The ε equation (turbulent dissipation rate equation) is as follows:

$$\frac{\partial \rho\varepsilon}{\partial t} + \frac{\partial\left(\rho u_j \varepsilon\right)}{\partial x_j} = \frac{\partial}{\partial x_j}\left[\left(\mu + \frac{u_t}{\sigma_\varepsilon}\right)\frac{\partial \varepsilon}{\partial x_j}\right] + G_{\varepsilon 1}\frac{\varepsilon}{\mathrm{k}}\left(G_k + c_{\varepsilon 3}G_b\right) - c_{\varepsilon 2}\rho\frac{\varepsilon^2}{k} + S_\varepsilon \tag{13}$$

3. Analysis of geometrical models

Because of the smaller cavity volume and bigger restriction clearance, the staggered labyrinth seal structure was selected as the study object. In the manufacturing process, the common seal structure materials include metal (such as aluminium or stainless steel), non-metallic materials (such as rubber, ceramic, or graphite), composite materials (such as rubber-asbestos or aerogel felt-polyurethane), and the most widely used material, rubber-like elastic material. The reliability of numerical simulation results depends on the correct application of key technologies. For example, the choice of mathematical model, numerical solution method, boundary conditions, and grid generation are all factors in obtaining accurate results. Five different sizes of tooth profile angles for staggered labyrinth seal structures, including 15°, 30°, 45°, 60°, and 75°, were studied. The piston velocity was set as v = 4.25 mm/s, seal clearance was H, and space widths were B_1 and B_2 while the cavity depths T_1 and T_2 were set as constants. The geometric parameter model and parameter sizes are listed in Figure 1 and Table 1, respectively. The solid model and 3D solid domain mesh of a piston are shown in Figure 2, and Table 2 lists the cylinder boundary conditions.

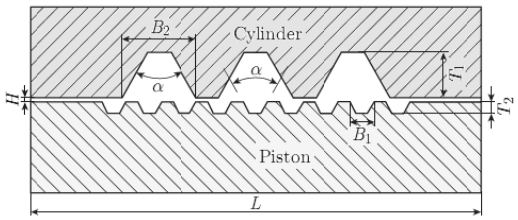

Figure 1. Geometric parameters of the model.

The boundary conditions of the solid surface were set without the slippage or permeation and acted as the adiabatic wall. The kinetic fluid field adopted the spring-based smoothing and reconstruction

model of the local grid to renovate the dynamic mesh. Gambit 2.0 was used to generate the unstructured grids in the labyrinth channels. However, the local grid reconstruction model can only be used for a tetrahedron grid or triangular grid, so the former was used for the 3-D fluid domain and solid structure grid.

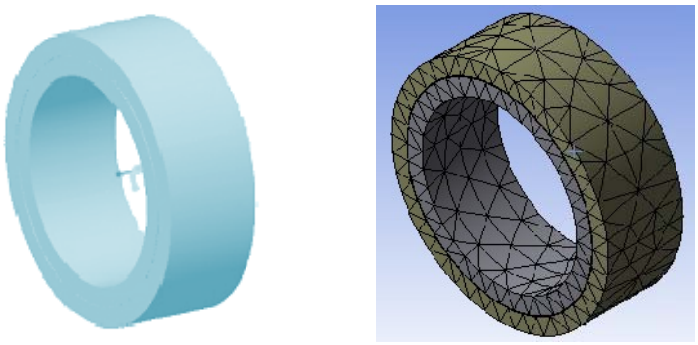

a. Solid model b. 3D solid domain mesh

Figure 2. Models of piston and cylinder.

Table 1. Geometrical parameters of the sealed cavity.

Cylinder teeth /n_1	Piston teeth /n_2	Seal clearance /H (mm)	Cylinder cavity depth /T_1 (mm)	Piston cavity depth /T_2 (mm)	Sealing length /L (mm)	Piston cavity width /B_1 (mm)	Cylinder cavity width /B_2 (mm)	Piston radius /R (mm)
3	9	0.4	4	1	40	2.15	6.5	50

Table 2. Boundary conditions of the model.

Working medium	Specific heat at constant pressure J/(kg·K)	Thermal conductivity W/(m·K)	Inlet of model	Outlet of model	Temperature (K)	Behavior of gas
Ideal gas	1006.43	0.0242	Given total pressure	Backpressure environment	300	Compressible gas

4. Analysis of calculation results

4.1. Tooth angle influence on leakage rate

Tooth shape is an important parameter affecting labyrinth seal structure, and the most common cavity tooth form of labyrinth seals in engineering are the triangle labyrinth seal, trapezoidal seal tooth, rectangular seal tooth, and stepped seal tooth. The trapezoidal labyrinth seal tooth, offering outstanding performance and simple machine processing, has been widely applied in engineering fields. Focused on the isosceles trapezoid tooth, the five different sizes of labyrinth seal structure teeth of 15°, 30°, 45°, 60°, and 75° were respectively discussed. With simulation analyses, Figures 3-7 illustrate the turbulence kinetic energy and total displacement nephogram for each tooth angle of the 3-D flow field. It can be seen that the amount of structure deformation showed an initial decline, followed by an increase with the degree of tooth angle. When the configuration size was fixed, the formation of the cavity eddy current was facilitated with the degree of the tooth angle. In the shear at the junction between the jet flow and backflow, the turbulence kinetic energy also showed an increasing trend, and the energy conversion was subsequently enhanced. It was observed that the strongest whirl vortex appeared in the expansion cavity at the seal tooth profile angle of 60°. The energy dissipated completely, and the seal leakage rate was the lowest. At the extreme tooth profile

angle, the conversion between the kinetic energy and heat energy in the expansion cavity was relatively weak, and the leakage rate increased significantly at that moment. In conclusion, both the energy dissipation of the subject vortex in the expansion cavity and energy exchange at the throttling gear had significant effects on the improvement of the seal leakage rate, and the former was more apparent. Different tooth profile angles of labyrinth seal leakage are listed in Figure 8 along with simulation and iterative calculations.

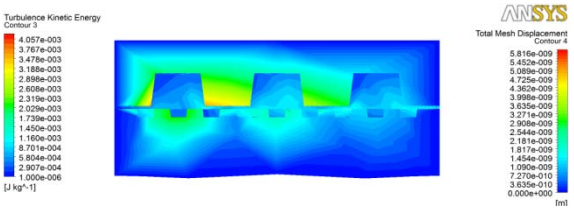

Figure 3. Turbulence kinetic energy and total mesh displacement nephogram with tooth angle of 15°.

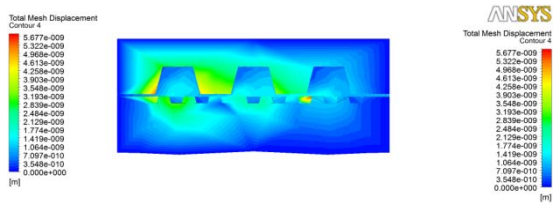

Figure 4. Turbulence kinetic energy and total mesh displacement nephogram with tooth angle of 30°.

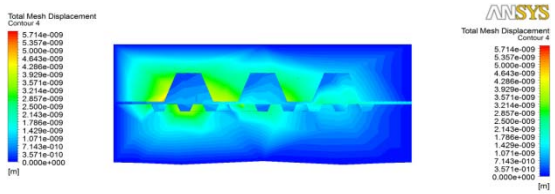

Figure 5. Turbulence kinetic energy and total mesh displacement nephogram with tooth angle of 45°.

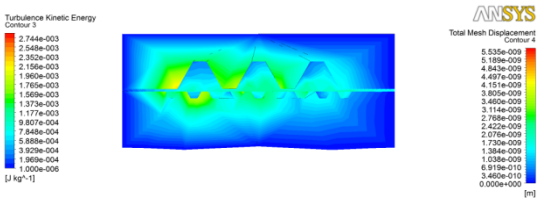

Figure 6. Turbulence kinetic energy and total mesh displacement nephogram with tooth angle of 60°.

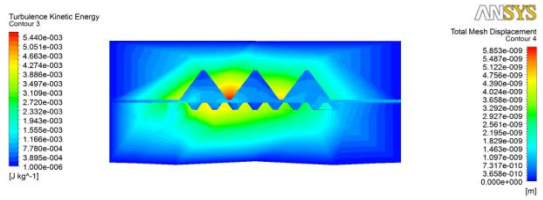

Figure 7. Turbulence kinetic energy and total mesh displacement nephogram with tooth angle of 75°.

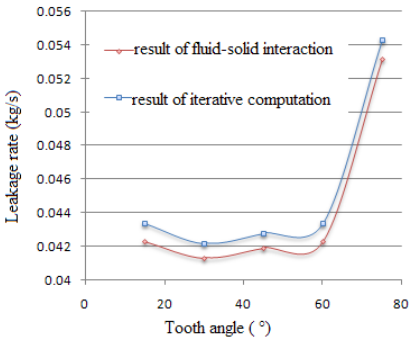

Figure 8. Leakage rate of labyrinth seal with the degree of tooth angles.

When the tooth angle was between 15° and 30°, the leakage decreased gradually, and between 30° and 60°, the leakage increased gradually. However, from 60° to 70°, the leakage increased sharply. The leakage was the lowest at the tooth profile angle of 30°. The major forms of fluid flow within the seal chamber were the main vortex and the jet, which were important factors resulting in energy loss. Energy loss was also related to the formation of small local vortexes in the shear layer of the strong jet and the merging primary vortex, jet impingement against the sealed wall, changes of jet direction, and other factors. When the jet flowed through the orifice, deflection flows directly impacted on the cavity wall, which caused kinetic energy loss; jet branches were thus produced. At the appropriate tooth profile angles, the jet velocity in the seal clearance decreased gradually with the degree of tooth angle, and most of the fluid energy dissipated completely after the long seal clearance. If the tooth angle was too wide, the flow velocity was accelerated into the cavity and the corner position, so the leakage rate decreased.

4.2. Comparison of leakage rate with the sealing clearance

The size of the sealing clearance has significant effects on labyrinth seals. For labyrinth compressors, too-wide seal clearance increases leakage, and thus reduces the efficiency of the compressor. Too-narrow seal clearance gives rise to difficulty in the manufacturing process, and the material performance requirements of labyrinth pistons are also strict. Figures 9-13 illustrate the turbulence kinetic energy and total mesh displacement nephogram for different sealing clearances.

As the figures demonstrate, labyrinth seal leakage increased with the widening of sealing clearance. Because the wider sealing clearance affected the resistance of the labyrinth seal, the ability of gas to convert pressure energy to kinetic energy was weakened, and the speed at which it entered the seal cavity in jet form dropped. With the turbulent kinetic energy of the gas in sealed cavity weakened, the energy dissipation of the gas decreased, and consequently, the leakage rate increased.

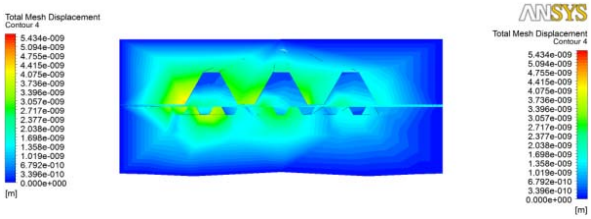

Figure 9. Turbulence kinetic energy and total mesh displacement nephogram (gap of 0.3 mm).

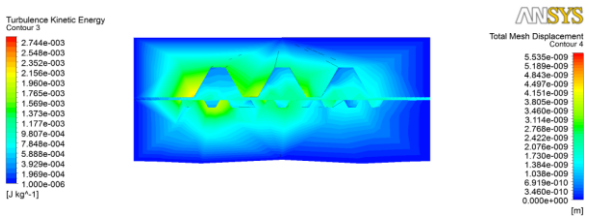

Figure 10. Turbulence kinetic energy and total mesh displacement nephogram (gap of 0.4 mm).

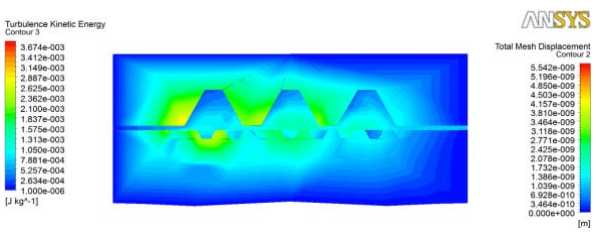

Figure 11. Turbulence kinetic energy and total mesh displacement nephogram (gap of 0.5 mm).

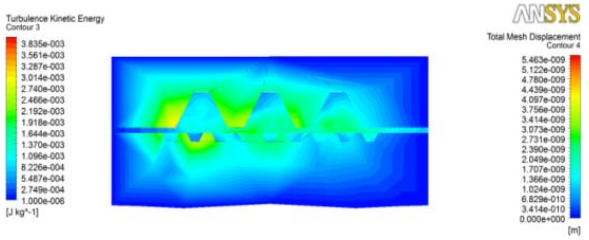

Figure 12. Turbulence kinetic energy and total mesh displacement nephogram (gap of 0.6 mm).

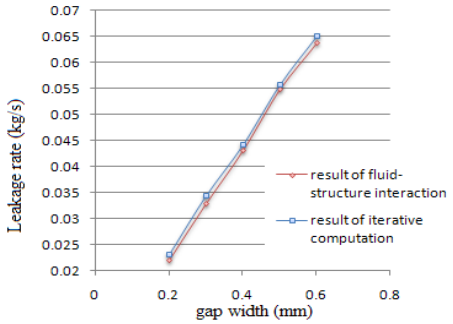

Figure 13. Labyrinth seal leakage for different sealing clearances.

4.3. Effects of leakage rate on the cavity depth

The configuration of fluid load can be affected by cavity depth, which changes the fluid leakage rate and the sealing effect. A smaller depth not only causes difficulty in the manufacturing process, but the performance requirement of labyrinth piston material is becoming more strict. Figures 14-19 illustrate pressure and von mises stress nephogram with different cavity depths. With a gradual increase of cavity depth, the wall deformation of the seal increased at first, then decreased to a certain point, and lastly, demonstrated a gradual increasing trend. It can be seen that the minimum leakage rate occurred at the cavity depth of 3.5-4 mm, during which time optimal sealing effect was obtained. When the

airflow through the throttling cavity, mainly by direct jet, and the flow with a certain angle entered the sealed cavity, a vortex inside the sealed cavity was generated, exacerbating the conversion from kinetic energy into heat energy, and causing the energy to dissipate. For a smaller cavity depth, most of the fluid was in the form of a jet flow, which did not easily form a vortex, and as a result, the cavity fluid was rendered nearly motionless.

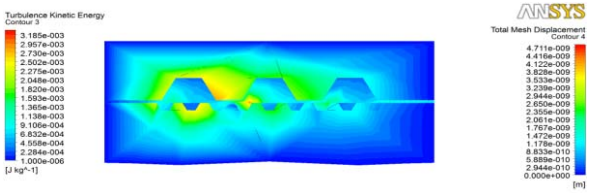

Figure 14. Turbulence kinetic energy and total mesh displacement nephogram (cavity depth of 3 mm).

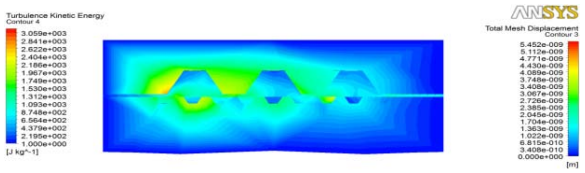

Figure 15. Turbulence kinetic energy and total mesh displacement nephogram (cavity depth of 3.5 mm).

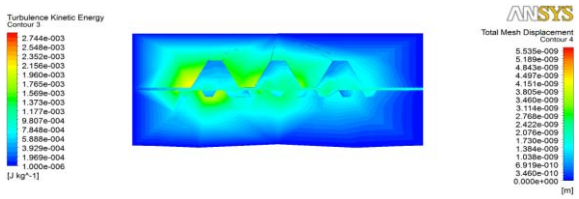

Figure 16. Turbulence kinetic energy and total mesh displacement nephogram (cavity depth of 4 mm).

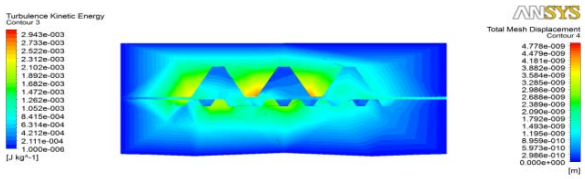

Figure 17. Turbulence kinetic energy and total mesh displacement nephogram (cavity depth of 4.5 mm).

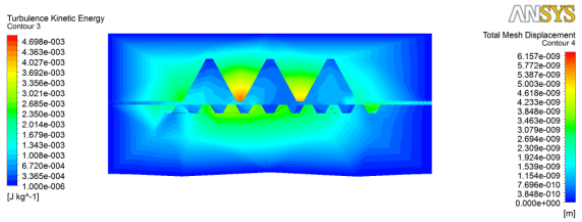

Figure 18. Turbulence kinetic energy and total mesh displacement nephogram (cavity depth of 5 mm).

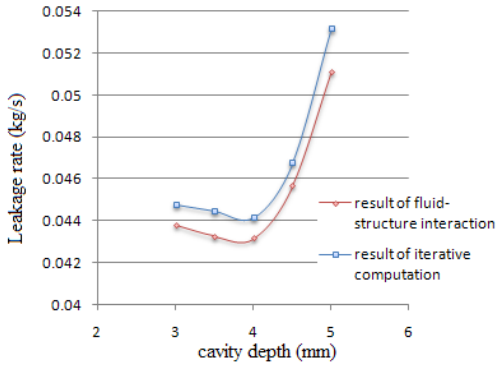

Figure 19. Labyrinth seal leakage for different cavity depths.

5. Conclusion

A numerical simulation model was established in this paper using the CFD analysis method, and the effects of the main labyrinth seal parameters, including tooth angle, sealing clearance, and cavity depth, were researched. After comparing the leakage rates between the fluid-structure interaction simulation and the experience formula calculations, the results revealed the validity of the fluid-structure interaction analysis method for labyrinth seals. In the future, the fluid-structure coupling can be adopted to verify the theory of labyrinth seals and to design labyrinth structures. The conclusions of the present study were drawn as follows:

(1) With the degree of tooth angle, the value of the leakage rate had a tendency to decrease at first, and then increase, according to fluid-solid coupling analysis. The lowest seal leakage rate occurred with a tooth profile angle of 60°.

(2) Labyrinth seal leakage increased with the increase of sealing clearance width. A smaller sealing clearance width should be adopted, but at the same time, reducing the difficulty of the manufacturing process should also be considered.

(3) For this type of reciprocating compressor, the minimum leakage was obtained at the cavity depth of 3.5 to 4 mm, when the sealing effect was the best.

Acknowledgement
This study was supported by Program for Collaborative Innovation Center of Major Machine Manufacturing in Liaoning, National Natural Science Foundation of China (Grant No. 61573249), and National Natural Science Foundation of China (Grant No. 51505298).

References

[1] Larjola J, Honkatukia J and Sallinen P *et al* 2010 Fluid dynamic modeling of a free piston engine with labyrinth seals *Journal of Thermal Science* **19**(2) 141-147
[2] Wu D Y 2000 Analysis and comparison of two commonly used labyrinth seal and critical features *Journal of Aerospace Power* **12**(4) 397-400
[3] Hu D X, Jia L and Yang L X 2014 Dimensional analysis on resistance characteristics of labyrinth seals *Journal of Thermal Science* **23**(6) 516-522
[4] Wang S F, Lv H F and Xia D Y 2004 Numerical analysis and experimental research of seal labyrinth structure features *Journal of Nanjing University of Aeronautics and Astronautics* **36**(6) 732-735
[5] Huang S L, Wang Z Y and Ma D W 2000 Flow analysis influence of cavity inclination on labyrinth leakage *Journal of Propulsion Technology* **16**(2) 40-45
[6] Liu Y J 2002 Study on sealing mechanism of a crenellated radial labyrinth seal *Lubrication Engineering* **154**(6) 20-21
[7] Li L and Liu W H 2007 Study of mechanism of labyrinth seal based on FLUENT *Chinese Mechanical Engineering* **18**(9) 2183-2186
[8] Versteeg H K and Malalasekera W 1995 *An Introduction to Computational Fluid Dynamics: The Finite Volume Method* (New York: Wily) pp 180-182
[9] Demko J A, Morrison G L and Rhode D L 1989 The prediction and measurement of compressible flow in a labyrinth seal *ASME Journal of Engineering Gas Turbines Power* **111**(4) 697-702
[10] Rhode D L and Sobolik S R 1986 Simulation of subsonic flow through a generic labyrinth seal *ASME Journal of Engineering Gas Turbines Power* **108** 674-680
[11] Zhu G T and Liu W H 2006 Analysis of calculational methods on leakage for labyrinth seals *Lubrication Engineering* **31**(4) 123-126
[12] Lin L 2007 Theory Study of the seal mechanism of labyrinth piston compressor Nanjing University of Aeronautics and Astronautics